

RESEARCH

Open Access



# Matrix Metalloproteinase-9 is associated with tumor microenvironment remodeling of bladder cancer

Fang Fang<sup>1†</sup>, Tiange Wu<sup>2†</sup>, Mengxue Wang<sup>2†</sup>, Wenchao Li<sup>3\*</sup>, Zonghao You<sup>3\*</sup>, Ming Chen<sup>3\*</sup> and Han Guan<sup>4\*†</sup>

## Abstract

Tumor microenvironment (TME) takes an essential part in the bladder cancer progression, which is associated with intercellular cross-talk between stroma cells and cancer. We aimed use bioinformatics tools to analyze tumor microenvironment remodeling in bladder cancer. CIBERSORT and ESTIMATE are bioinformatics tools based on deconvolution for calculating proportions of tumor-infiltrating immune cells and stromal components in TME. We utilized these two algorithms to analyze the immune components of 433 bladder cancer cases from The Cancer Genome Atlas database, aiming to compensate for the current lack of large-sample single-cell information. Then we used Cox regression to analyze the prognostic value of differentially expressed genes, and the protein–protein interaction network was constructed. Matrix Metalloproteinase-9 (MMP9) was identified as a predictive biomarker related to immune microenvironment. Using Gene Set Enrichment Analysis, the genes from the group with high MMP9 expression gathered in items related to immune diseases, and genes in the group with low MMP9 expression were negatively associated with valine, leucine and isoleucine degradation and glycosylphosphatidylinositol anchor biosynthesis. MMP9 expression and presence of macrophages M0 were positively correlated, while naïve B cells, activated dendritic cells, monocytes and plasma cells were negatively correlated. The results were confirmed by brightfield and multiplex fluorescence immunohistochemistry using stained bladder cancer and normal tissue.

**Keywords** Tumor microenvironment, Matrix Metalloproteinase-9, Tumor-infiltrating immune cells, Bladder cancer, Bioinformatics

<sup>†</sup>Fang Fang, Tiange Wu and Mengxue Wang contributed equally to this work.

\*Correspondence:

Wenchao Li  
3337847348@qq.com  
Zonghao You  
3075818401@qq.com  
Ming Chen  
mingchenseu@126.com

Han Guan  
51706@bbmc.edu.cn

<sup>1</sup>Department of Immunology, School of Laboratory Medicine, Anhui Province Key Laboratory of Immunology in Chronic Diseases, Bengbu Medical University, Bengbu, China

<sup>2</sup>Medical School of Southeast University, Nanjing, China

<sup>3</sup>Department of Urology, Affiliated Zhongda Hospital of Southeast University, Nanjing 210009, China

<sup>4</sup>Department of Urology, The First Affiliated Hospital of Bengbu Medical University, Bengbu 233030, China



## Introduction

Bladder cancer (BLC), which is one of the leading urogenital malignancies, ranks as the 9th most popular cancer in the world and the 13th highest mortality in all types of cancer [1]. It accounts for approximately 4% of all new cancer diagnoses in the United States and is responsible for an estimated 16,840 deaths annually [2]. Treatment options for BLC include cystectomy, immunotherapy, bladder preservation followed by chemotherapy and radiation, among others [3]. However, the overall survival rate is 66% at 5 years for patients undergoing radical cystectomy and extensive lymph node dissection, and only 50% for those receiving bladder preservation therapy [4]. Therefore, further exploration of the carcinogenesis and therapeutics of BLC is essential.

Previous studies have shown that the tumor microenvironment (TME) plays a crucial role in tumor progression, involving factors such as the immune microenvironment and intercellular communication between stromal cells and cancer cells [5, 6]. The TME functions at all stages of tumor progression, including cell invasion, extravasation, survival, and growth [7]. Research suggests that the TME significantly influences treatment response and clinical outcomes for patients, with tumor-infiltrating immune cells (TICs) in the TME reported to be associated with survival in patients with BLC, leading to improvements in immune-based therapeutics [8, 9]. However, despite the benefits reported from checkpoint inhibitor therapy, there are opportunities to improve response rates and treatment outcomes [10].

We deconvoluted the constituents of TICs and distinguished stromal and immune components in BLC samples from The Cancer Genome Atlas (TCGA). Matrix Metalloproteinase-9 (MMP9), one of the calcium-dependent, zinc-containing endopeptidases [11], was identified as a predictor for TICs and prognosis. MMP9 has gained increasing attention due to its correlation with the tumor microenvironment and angiogenesis. A previous study suggested that tissue-infiltrating neutrophils might be an important source of MMP9 in the TME [12]. Additionally, it has been reported that the invasion of BLC cells can be promoted by epithelial-mesenchymal transition through increased expression of MMP9 [13]. Therefore, we conducted this research by comparing immune and stromal components in BLC samples to confirm that MMP9 might indicate TME remodeling based on TCGA data mining.

## Materials and methods

### Raw data acquisition

A total of 433 BLC cases (19 normal samples, 414 tumor samples) and corresponding clinical characteristics data were obtained from the TCGA database (<https://portal.gdc.cancer.gov/>) [14].

### Survival analysis

Survival analysis was conducted using the R packages ‘survminer’ (<https://cran.r-project.org/web/packages/survminer/>) and ‘Survival’ (<https://cran.r-project.org/web/packages/survival/>) in R version 3.5.1 (<https://cran.r-project.org/>). Univariate Cox regression was used to evaluate the prognostic value of immune-related genes. The survival curve was generated using the Kaplan-Meier method, and the *p*-value was calculated using the Log-rank test, with significance set at  $<0.05$ .

### Generation of tumor microenvironment scores

ImmuneScore, StromalScore, and EstimateScore are metrics derived from bioinformatics algorithms that provide insights into the tumor microenvironment (TME) and its composition in the context of cancer. These scores are positively associated with the proportion of immune, stromal components, and their combined total, respectively. ImmuneScore, StromalScore, and EstimateScore were generated using the R package ‘estimate’ (<https://r-forge.r-project.org/>), with the ESTIMATE algorithm being employed [15].

### Generation of differentially expressed genes

Classified with the median score of ImmuneScore and StromalScore, 414 tumor samples were divided into two groups expressing high and low MMP9 respectively. Differential gene expression analysis was conducted using the R package ‘limma’ (<https://cran.r-project.org/web/packages/limma/>). Differentially expressed genes (DEGs) were transformed using  $\log_2$  (high-score group/low-score group), with significance set at  $>1$ . The false discovery rate (FDR) was considered statistically significant if  $<0.05$ .

### Pathway enrichment analyses

Gene Ontology (GO) [16] and Kyoto Encyclopedia of Genes and Genomes (KEGG) [17] enrichment analyses were performed using the R packages enrichplot, clusterProfiler, and ggplot2. Results were considered significant when both *p*- and *q*-values were  $<0.05$ .

Gene Set Enrichment Analysis (GSEA) was conducted using Hallmark and C7 gene sets downloaded from the Molecular Signatures Database (<https://www.gsea-msigdb.org/gsea/msigdb/human/>). Results were considered significant if NOM  $p < 0.05$  and FDR  $< 0.06$  in gene sets.

### Difference analysis in scores based on clinical stages

Samples were grouped based on clinical stages and pathological stages, including clinical stage I-II vs. stage III-IV, pathological T0-2 vs. T3-4, as well as pathological  $N \geq 1$  vs. N0. Differential analysis was conducted using R tools, with the Wilcoxon test used for significance testing.

### Heatmaps

The R package ‘pheatmap’ (<https://cran.r-project.org/web/packages/pheatmap/>) was used to generate heatmaps to display the expression profiles of the top 100 most significantly DEGs between the two groups in each comparison method, based on the RNA-seq data from TCGA BLC samples.

### Construction of protein–protein interaction network

For network reconstruction, we used the STRING database (<https://string-db.org/>) [18] and Cytoscape software [19], version 3.6. In the network construction, protein nodes were selected based on a criterion where the confidence of their interactive relationships exceeded 0.95 (Confidence threshold of 95%). This ensured that only interactions with a high level of certainty were included in the network analysis, providing a robust and reliable representation of the relationships between the proteins.

### Tumor-infiltrating immune cells profile

The assessment of the tumor-infiltrating immune cells (TICs) abundance profile in all tumor samples was conducted by CIBERSORT algorithm, using ‘CIBERSORT’ R package (<https://github.com/MoonerSS/CIBERSORT>) [20]. Using gene expression data from RNA-seq of BLC sample from TCGA and referring datasets that contain gene expression profiles of 22 pure immune cell populations (B cell naïve, B cell memory, Plasma cells, T cells CD8, T cells CD4 naïve, T cell CD4 memory resting, T cells memory activated, T cells follicular helper, Tregs, T cells gamma delta, NK cells resting, NK cells activated, Monocytes, Macrophages M0, Macrophages M1, Macrophages M2, Dendritic cells resting, Dendritic cells activated, Mast cells resting, Mast cells activated, Eosinophils and Neutrophils), we applied deconvolution algorithm of machine learning to estimate the relative proportions and abundance of each cell type in the tissue of interest.

### Immunohistochemistry (IHC) and multiplex fluorescence IHC

BLC tissues and adjacent normal bladder tissues were obtained from ex vivo specimens after radical cystectomy. All patients signed an informed consent form authorizing the use of surgical specimens for the study. The specimens were embedded in paraffin and sectioned for IHC testing. Postoperatively, BLC ( $n = 10$ ) and normal tissue ( $n = 2$ ) from 10 different patients were stained using brightfield and multiplex fluorescence IHC. The 4  $\mu\text{m}$  cut of tissue sections was used for IHC. For brightfield, tissue sections were dewaxed and incubated for 5 min in an autoclave at 121 °C in Tris-EDTA pH 7.8 antigen retrieval solution. Endogenous peroxidase was blocked, and antibodies were incubated. For multiplex fluorescence IHC, antibody staining was conducted in several procedures,

including peroxidase blocking, primary antibody application, secondary HRP-conjugated antibody testing, fluorescence dye testing, and microwave application to remove bound antibodies. Three different antibodies were stained three times in each experiment. Slides were then counterstained with diamidino-2-phenylindole (DAPI) and mounted in antifade solution.

The specifications of all antibodies used and the criteria for positive IHC score are listed as follows:

Antibodies: MMP9, GB11132, Servicebio, 1:1000; CD14, GB11254, Servicebio, 1:500; CD138, ab128936, Abcam, 1:1000; CD19, GB11061, Servicebio, 1:800; CD11c, GB11059, Servicebio, 1:400; CD168, GB113109, Servicebio, 1:400.

Criteria: (a) No staining as 0, weak as 1, moderate as 2, and 3 for strong staining; (b) score 1 if less than 25% of cancer cells were stained, 25–75% as 2, and more than 75% as 3. The final score was recorded as sum of both scores, and the tissue core was recognized as positively stained if the final score was more than 4.

## Results

### Analysis process

A total of 433 BLC cases with transcriptome RNA-seq data were acquired to accomplish the calculation of the TICs proportion and the ratio of immune and stromal parts with the use of TCGA database. The ESTIMATE algorithm was utilized to calculate the ImmuneScore, StromalScore, and EstimateScore for each sample of BLC from TCGA, in order to assess the infiltration of overall immune cells and stromal cells in the samples. Based on the median scores, enriched and depleted immune infiltration phenotypes were inferred, and samples were grouped accordingly for subsequent differential gene screening. On the other hand, the CIBERSORT algorithm was employed to deconvolute the infiltration abundance and proportion of 22 immune cell populations for each case, to evaluate the correlation between the genes of interest and the infiltration of various types of immune cells. Protein–protein interaction (PPI) network and univariate Cox regression analysis were constructed using differentially expressed genes (DEGs). The main nodes achieved from PPI network and critical factors in the analysis of Cox regression were used to perform the intersection analysis. As a result, MMP9 was chosen for the subsequent analysis, including the association between clinicopathological characteristics and survival, GSEA, Cox regression, as well as the relation with TICs. The whole analysis process is concluded and shown in Fig. 1.

### Survival rate was associated with scores in BLC patients

Kaplan-Meier survival analysis was conducted in ImmuneScore, StromalScore, and EstimateScore respectively

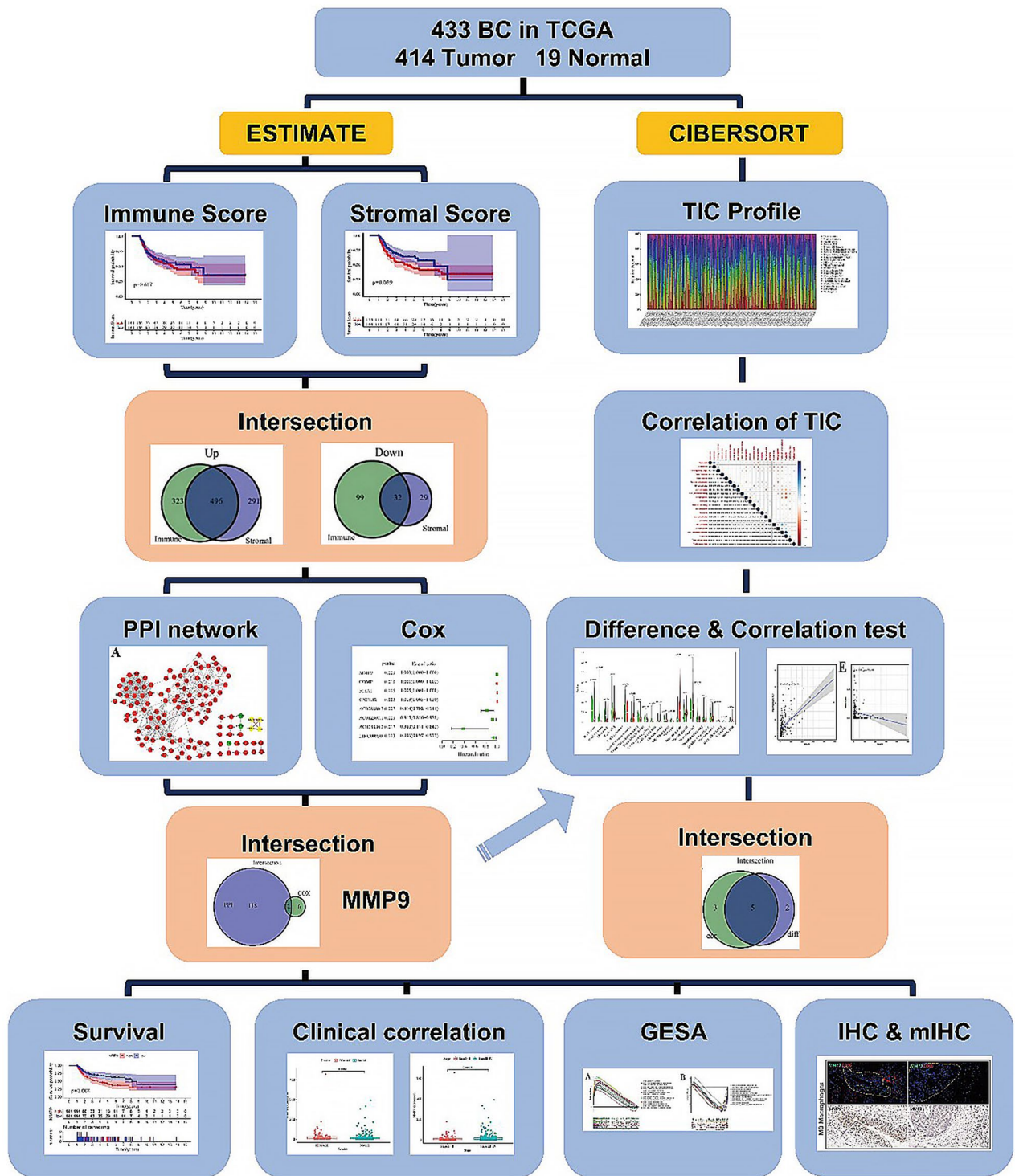


**Fig. 1** Analysis workflow of this study

to search for the relation between the immune and stromal components and the survival results of BLC patients. EstimateScore was the comprehensive proportion of two parts in TME, summing up ImmuneScore and StromalScore. Based on the Kaplan-Meier analyses, we found

that BLC patients with higher StromalScore have poorer overall survival (Log-rank  $p=0.039$ ), while the ImmuneScore (Log-rank  $p=0.617$ ) and EstimateScore (Log-rank  $p=0.088$ ) had no significant association with the overall survival (Fig. 2A-C).

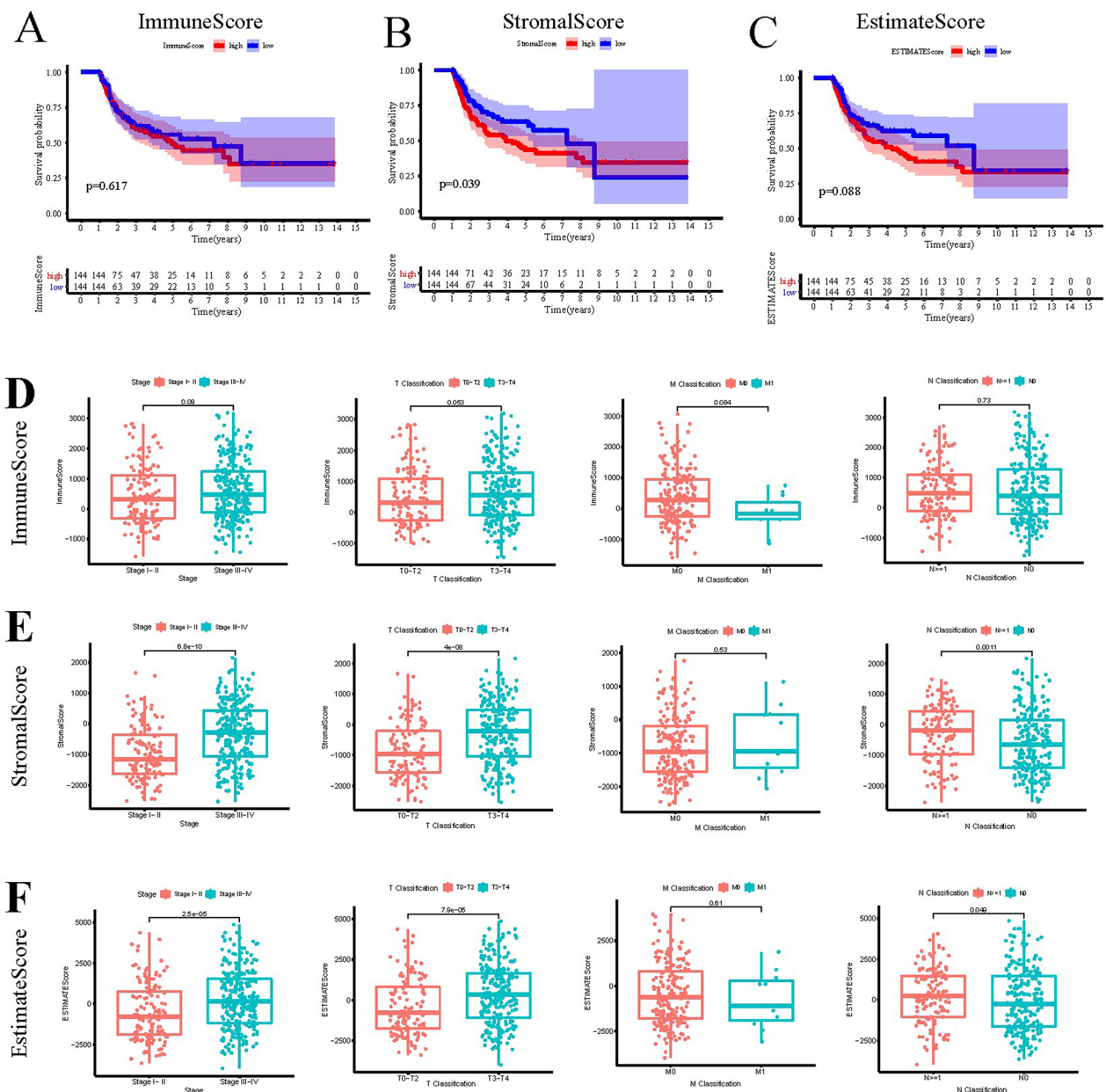


**Fig. 2** Association between scores and the prognosis of BLC patients. **(A)** Kaplan–Meier survival analysis for ImmuneScore in BLC patient with different scores.  $p=0.617$ . **(B)** Survival analysis of Kaplan–Meier for StromalScore with  $p=0.039$ . **(C)** Kaplan–Meier survival curve for ESTIMATEScore with  $p=0.088$ . **(D)** Association between ImmuneScore and staging characteristics in clinicopathology by Kruskal–Wallis rank sum test. **(E)** Correlation of StromalScore with clinicopathological staging characteristics by Kruskal–Wallis rank sum test. **(F)** Correlation of ESTIMATEScore with clinicopathological staging characteristics by Kruskal–Wallis rank sum test

**Clinic-pathological staging was related to scores in BLC samples**

The clinical information of BLC patients accordingly was obtained from TCGA to determine the whether the proportion of immune and stromal parts is associated with the clinicopathological characteristics. It showed that StromalScore was higher in clinical stage III-IV than that in clinical stage I-II ( $p=6.8e-10$ ), and it was also higher

in advanced pathological T3-4 stage ( $p=4e-8$ ) and pathological  $N \geq 1$  stage ( $p=0.0011$ ) (Fig. 2E), indicating the stromal part in BLC may related to progressive clinical features. What’s more, we also found that higher EstimateScore was established in advanced clinical stage ( $p=2.5e-5$ ), higher pathological T stage ( $p=7.9e-5$ ) and higher pathological N stage ( $p=0.049$ ), which meant the overall distribution of cells in the microenvironment

could also indicate the clinical and pathological characteristics of BLC (Fig. 2F).

#### DEGs and enriched pathways of immune-related genes

The samples with high score and low score were compared, in order to investigate the precise alterations of gene profile in immune and stromal parts in TME. A total of 950 genes were gained from ImmuneScore, in which 819 were up-regulated genes while 131 were down-regulated (Fig. 3A, C). In terms of StromalScore, 848 genes were gained, and 787 of them were up-regulated and 61 were down-regulated (Fig. 3B, C). As shown Venn plot in Fig. 4C, there was an intersection in 496 up-regulated genes in both immune and stromal components, as well as 32 down-regulated genes. A total of 528 genes were possibly associated with TME was eventually screened. As were shown in the bubbleplot and barplot of GO pathway enrichment analysis, we found the DEGs functioned mainly in immune response, including activating cell surface receptor signaling pathway and signal transduction (Fig. 3D, F). In circleplot of GO, DEGs was considered to be related in immune response, complement activation, B cell mediated immunity (Fig. 3H). The bubbleplot, barplot and circleplot of KEGG enrichment analysis showed the gathering of cytokine receptor interaction (Fig. 3E, G, I).

#### PPI network and Cox regression

We conducted a PPI analysis on the 528 DEGs to construct a proteinic interaction network. In this network, each node represents a protein molecule, and each connecting line indicates an interaction between two proteins. Ultimately, based on the analysis, we identified 120 proteins that had more than two pairs of interaction relationships, forming a complex protein interaction network (Fig. 4A). Furthermore, we included the 528 DEGs in a univariate Cox regression analysis to identify prognostic factors. The results showed that high expression of MMP9, COMP, F13A1 and CXCL12 were associated with poor overall survival in BLC patients (Fig. 4B). After overlapping the prognosis-predictive genes and PPI-functional genes, MMP9 and CXCL12 were identified as two immune-related functional prognostic genes (Fig. 4C). Since that CXCL12 has been reported to be immune-related prognostic gene in BLC in a previous study [27, 28], MMP9 was chosen to be the target gene for subsequent analyses.

#### The associated between MMP9 expression and clinical characteristics in BLC patients

According to the expression of MMP9 compared with median expression in BLC samples, all the samples were divided into two groups with high-expression and low-expression MMP9. The survival analysis suggested that

BLC patients tended to have longer survival time in low-expression group (Fig. 4F). As the Wilcoxon rank sum test showed in Fig. 4D, the expression of MMP9 in tumor samples was distinctly higher compared with normal samples. The analysis was then conducted in the same patient, and the result was similar to before (Fig. 4E). Also, the expression of MMP9 was distinctly related to gender, tumor stage and T, N stage of BLC patients (Fig. 4G-K).

#### The correlation of MMP9 with TME and TICs

GSEA was performed in group with high MMP9 expression, and the results suggested that the genes in this group gathered in items related to immune diseases, including allograft rejection and graft versus host disease (Fig. 5A), and genes in the group expressing low MMP9 were negatively associated with valine leucine and isoleucine degradation and glycosylphosphatidylinositol anchor biosynthesis (Fig. 5B). Then, the CIBERSORT algorithm was applied in 22 types of immune cell profiles in BLC samples (Fig. 5C, D). Difference analysis was shown in Fig. 6A, and a total of 7 kinds of TICs were found significant. After the intersection analysis in difference and correlation tests, 5 kinds of TICs including B cells naïve, dendritic cells activated, macrophages M0, monocytes and plasma cells were found related to the expression of MMP9 (Fig. 6B). Among these TICs, macrophage M0 showed positive association to MMP9 expression and B cells naïve, dendritic cells activated, monocytes and plasma cells were on the contrary (Fig. 6C-G).

#### Immunohistochemistry (IHC) and multiplex fluorescence IHC

IHC showed that the expression of MMP9 differed in different patients (Fig. 7A). According to the results of fluorescence multiplex IHC, monocytes, B cells naïve, dendritic cells activated and plasma cells showed negative correlation with MMP9 expression, while the macrophage M0 had positive association with MMP9 expression (Fig. 7B, C), which were consistent with the results generated from database.

#### Discussion

In the present study, MMP9 was found to be correlated with the prognostic results and the classification of TNM stages in BLC patients, involving the immune activities. Previous studies demonstrated that MMP9 was related to tumor angiogenesis and metastasis in avascular tumors [21] and mediation of the progression and preservation of neovascular networks that sustain the tumor cell intravasation [22]. Tissue infiltrating neutrophils have been reported to be an essential source of MMP9 in TME [12].

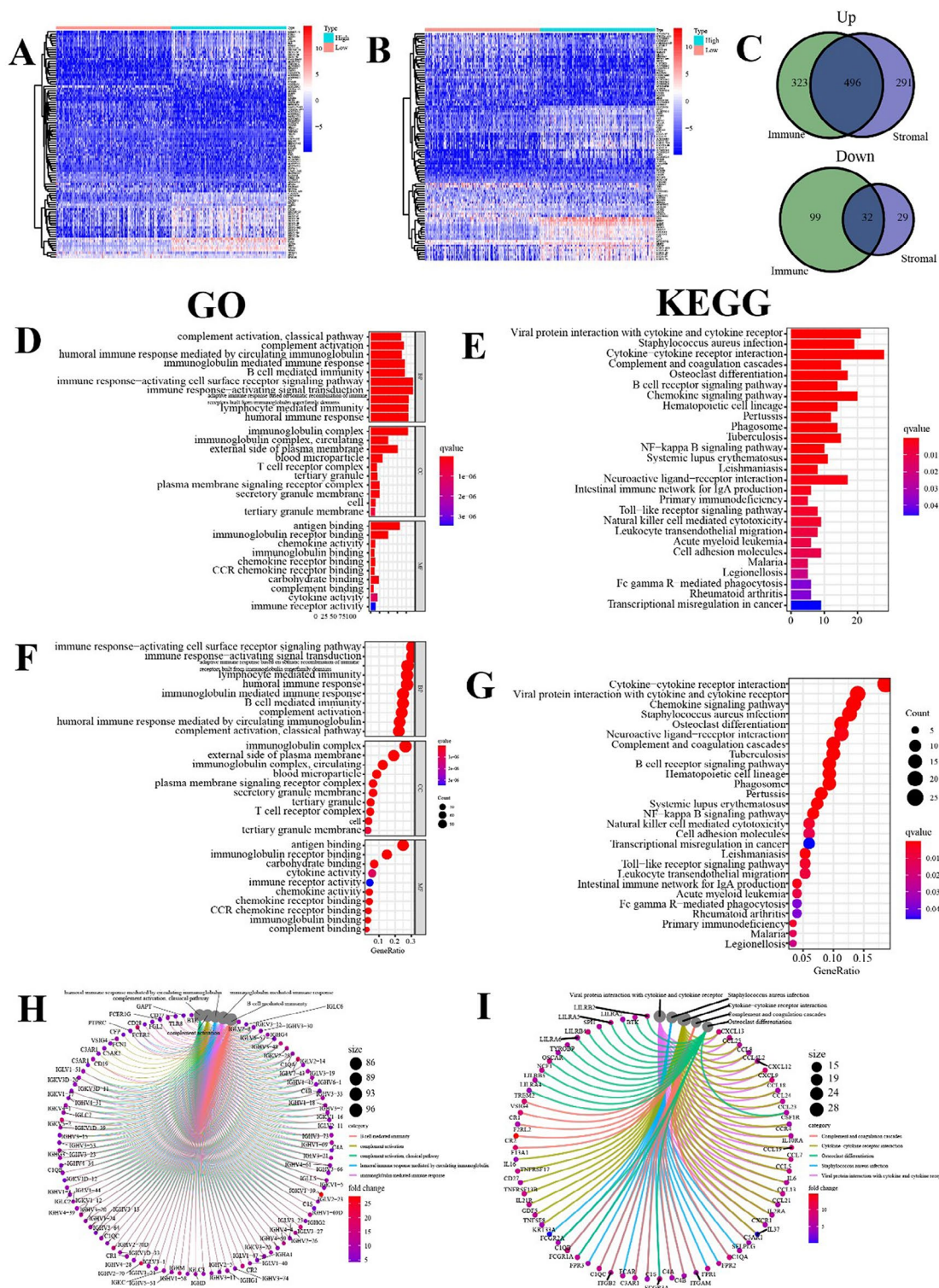


**Fig. 3** Analyses with the methods of gene ontology (GO) and Kyoto Encyclopedia of Genes and Genomes (KEGG) in DEGs. **(A)** Heatmap for DEGs acquired by comparing the different expression of ImmuneScore of genes in two groups, by Wilcoxon rank sum test. **(B)** Heatmap for DEGs generated by comparing the different expression of StromalScore of genes. **(C)** Venn plots of DEGs which were up-regulated or down-regulated in both ImmuneScore and StromalScore, terms with  $q < 0.05$  and  $q > 1$  after  $\log_2$  calculation were significant. **(D, F, H)** Enrichment analysis in Bubbleplot, Barplot and Circleplot of GO for 528 DEGs, and  $p$  and  $q < 0.05$  were the significance filtering threshold. **(E, G, I)** KEGG enrichment analysis in Bubbleplot, Barplot and Circleplot for 528 DEGs, and  $p$  and  $q < 0.05$  were the significance filtering threshold

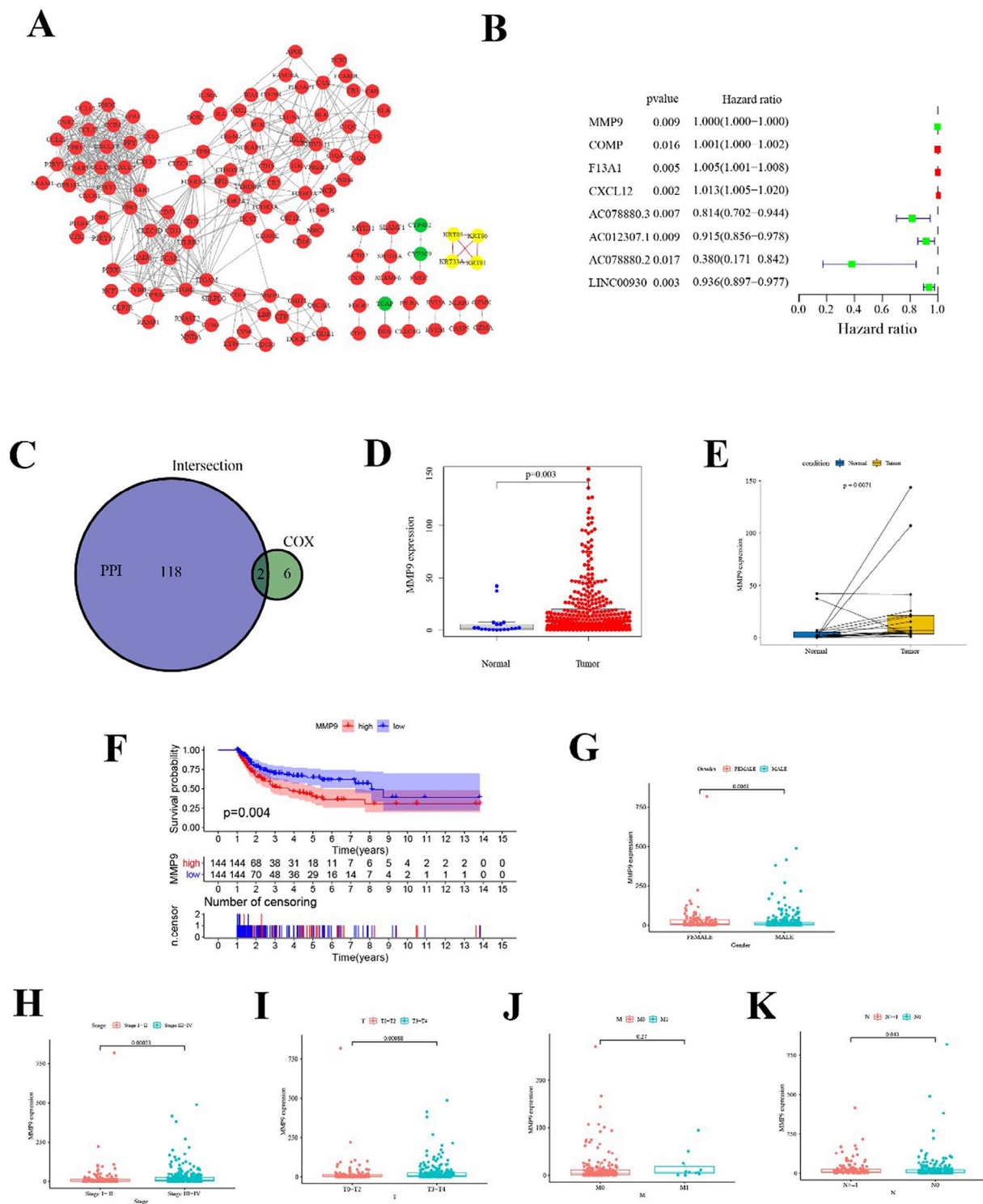


**Fig. 4** Protein–protein interaction network (PPI), Cox analysis for DEGs, MMP9 expressions in different samples and their association with prognosis and clinical characteristics of BLC patients. **(A)** PPI generated using the nodes whose interaction confidence value were beyond 0.95. **(B)** Univariate Cox regression analysis for 528 DEGs, and the most significant genes were listed. **(C)** Venn plot indicating the genes in both the top 120 nodes from PPI and most significant genes in Cox regression. **(D)** MMP9 expressions in the samples from all normal and BLC tissues. **(E)** MMP9 expressions in the samples from both normal and BLC tissues in one patient. **(F)** Association between prognosis and MMP9 expressions in BLC patients by survival analysis. **(F–K)** The association between the expressions of MMP9 and gender, as well as staging characteristics in clinicopathology, using Wilcoxon rank sum or Kruskal–Wallis rank sum test to set the significance filtering threshold

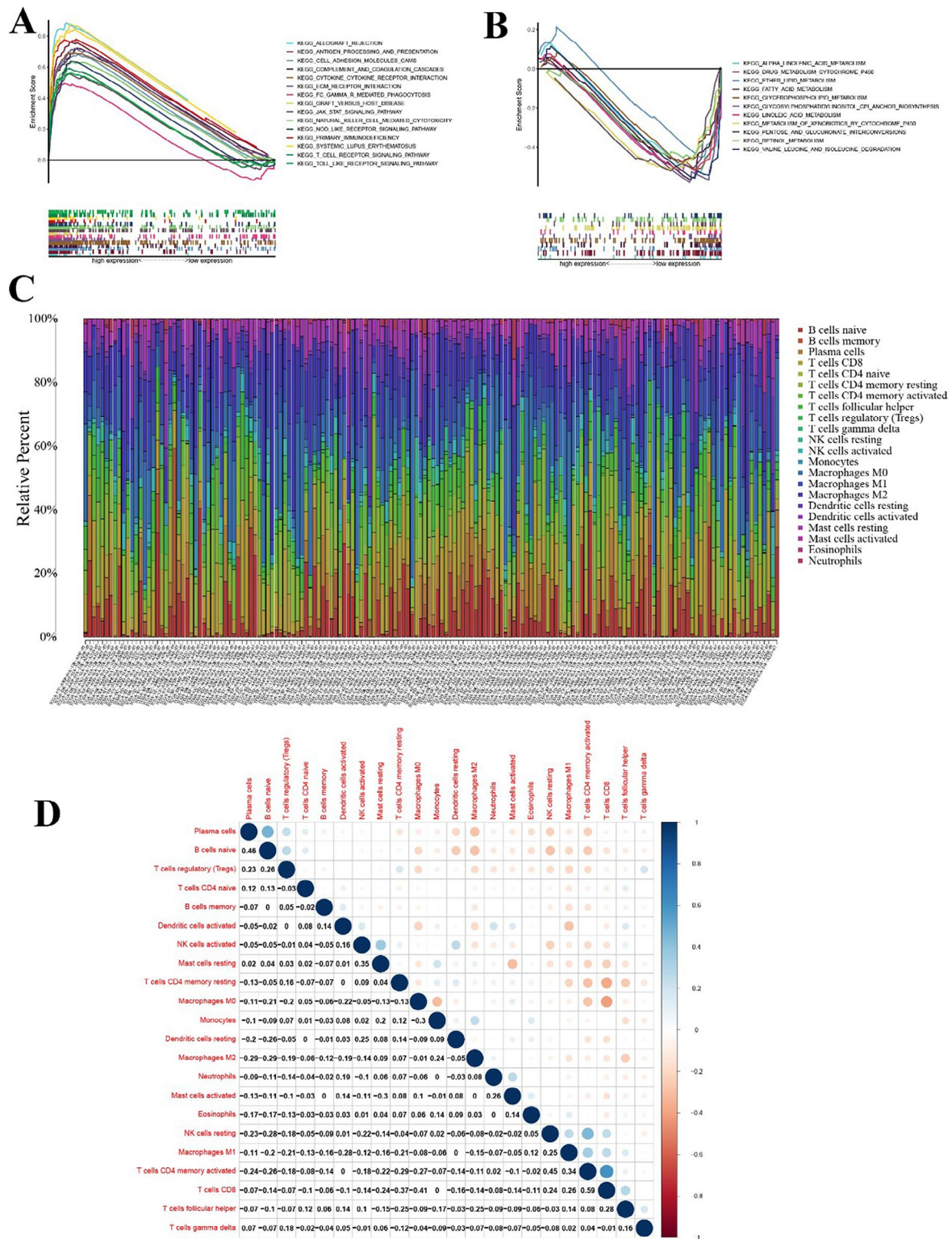


**Fig. 5** GSEA for normal and BLC tissues with different MMP9 expressions, TIC profile in tumor samples and correlation analysis. **(A)** The most leading gene-rich sets were shown in Hallmark [31] collection with samples highly expressing MMP9, and  $NOM p < 0.05$  and  $FDR < 0.06$  were set to be the significance filtering threshold. **(B)** The gene-rich sets in tissues expressing MMP9 lowly. **(C)** Barplot indicated the constitute of TICs in 22 types in BLC tissues. **(D)** Heatmap indicated the association of TICs. The figures represented the p value of association between two TICs. Pearson coefficient was chosen to set the significance filtering threshold

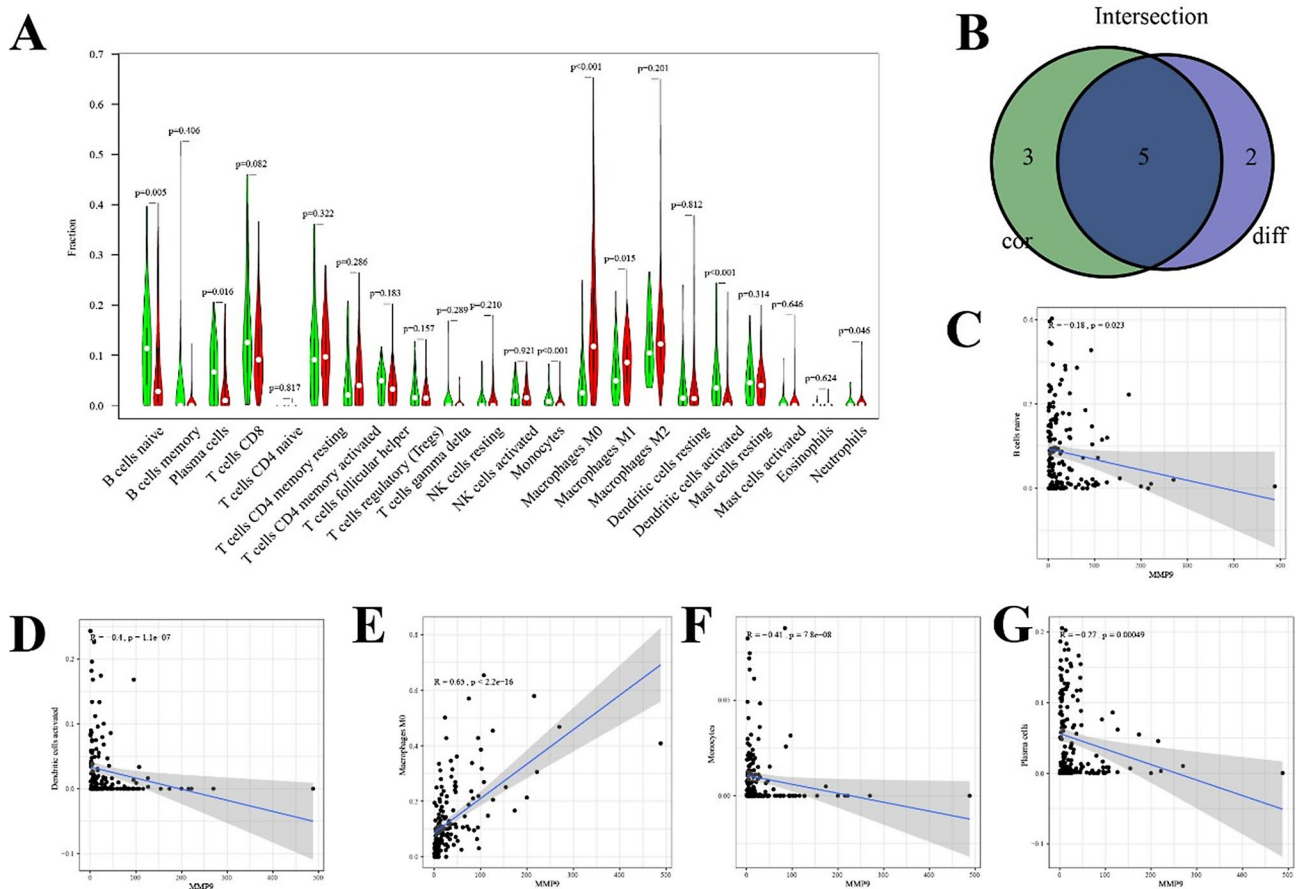


**Fig. 6** Association between TICs proportion and MMP9 expression. **(A)** Violin plot indicated the ratio differentiation of TICs between BLC tumor samples expressing MMP9 highly or lowly, and the significance filtering threshold was set by Wilcoxon rank sum. **(B)** Venn plot indicated five kinds of TICs associated with MMP9 expression using difference and correlation tests. **(C)** Scatter plot displayed the association between 5 kinds of TICs proportion and MMP9 expression ( $p < 0.05$ ). The blue line represented the proportion tropism of the TICs with MMP9 expression

ImmuneScore, StromalScore, and EstimateScore are crucial in the context of bladder cancer marker search as they offer a quantitative approach to characterize the TME. The differences in ESTIMATE scores between groups largely depend on the expression of tumor DEGs. Understanding the ImmuneScore and StromalScore in bladder cancer can help identify potential biomarkers associated with immune response and stromal interactions, which may predict patient outcomes and response to treatment. By analyzing these scores, researchers can uncover novel therapeutic targets and develop more effective treatment strategies tailored to the specific immune and stromal landscape of individual tumors. This approach aligns with the aim of the study to discover new bladder cancer biomarkers and understand the TME's role in disease progression and therapy response. In this study, the proportion of stromal parts was found to have negative correlation with overall survival rate. Consistent with the previous studies, evidence showed that the TME was related to tumor development and metastasis [23], in which the stromal cells such as

fibroblasts, are associated with the exocrine phenotype of T cells in tumor microenvironment [24]. DEGs from ImmuneScore and StromalScore were shown to be associated with immune response, which indicated the potential in immunotherapy. In cancer immunotherapy, there are two strategies, including improving the general immune response and inhibiting the immune suppressor functions. Bladder cancer patients benefit a lot from standard therapeutic methods, such as bacillus Calmette-Guérin (BCG) and anti-PD-1/PD-L1 immunotherapies, which makes BLC suitable for testing the immunotherapy [25]. In a previous review by McConkey et al., the infiltrated subtype, which is one of four molecular subtypes of muscle invasive bladder cancer, was reported to be sensitive to immune checkpoint inhibitors [26]. Thus, we started from the transcriptomic data of BLC from TCGA, and found that the increased expression of MMP9 was related to the more advanced clinical stages and poorer survival outcomes. In conclusion, it's shown that MMP9 could play the role as a potential prognostic indicator and a target for immunotherapy TME in BLC.

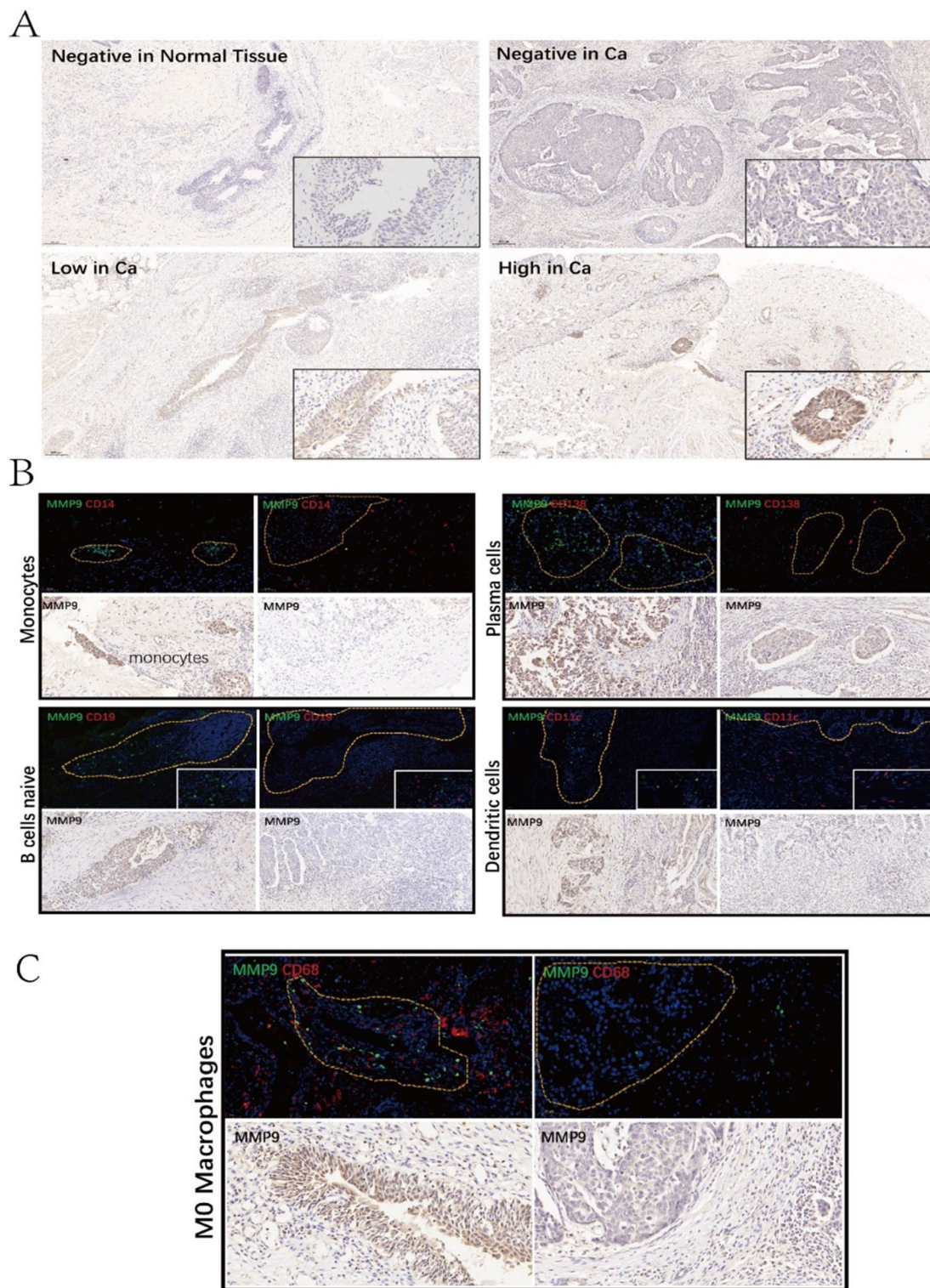


**Fig. 7** Correlation between MMP9 and TICs biomarkers in BLC and normal tissue specimens. **(A)** Immunohistochemistry (IHC) staining was used to analyze MMP9 expression in 1 normal tissue and 3 BLC specimens. **(B)** Multiplex fluorescence IHC was used to analyze the biomarkers of monocytes, plasma cells, B cells naïve and dendritic cells, and MMP9. **(C)** Multiplex fluorescence IHC was used to analyze the biomarker of M0 macrophages and MMP9

MMP9 is one of calcium-dependent, zinc-containing endopeptidases, which has proved to have relationship with tumor angiogenesis and metastasis, maintain the stability of distinct neovascular networks and sustain the tumor cell intravasation [19]. However, considering the previous failed clinical trials, there still exists limitations on clinical utility of broad-spectrum MMP inhibitors, leading to the demand for development of inhibitors selective for individual MMPs [27]. A previous study investigating the role of MMP9 in promoting breast cancer, found that MMP9 inhibition decreased tumor volume and suppressed metastases in obese mice significantly [28], which may not due to the direct interaction between MMP9 and tumor cells, but to do with microenvironment modulation. The cancer-promoting effects of MMP9 can be exerted with multiple mechanisms including degrading basement membranes [29], which inhibited the tumor invasion into surrounding tissues. In a study on recruited mast cells in TME in bladder cancer, it's shown that infiltrated mast cells in TME accelerate the metastases of BLC via stimulating ER $\beta$ /CCL2/CCR2 EMT/MMP9 signals both in vitro and vivo [13]. However, the association between MMP9 and TICs in TME is still not clear. V Juric et al. demonstrated that the combined inhibition of MMP9 and PD-L1 increased the tumoral infiltration of effector T cells and the diversity of TILs (PMID 30500835). However, no significant difference was found between in vivo anti-PD-L1 and combination treatment with anti-MMP9 in this study, which implies that there may be other mechanisms involved. A recent study found that the poor antigen-presenting cell status led to ineffective presentation of antigen to CD8+ T cells and included high infiltration of naïve B cells and low T follicular helper cell and dendritic cells activation, which resulted in poorer prognosis [30]. In our study, MMP9 was reported to be highly expressed, with considerable variability among individuals, in BLC compared to normal tissue, and positively related to B cells naïve, while it has negative correlation with dendritic cells activated, monocytes and plasma cells. Therefore, the positive association between B cells naïve and MMP9, and the negative association between dendritic cells and MMP9 might be responsible for the poor prognosis in patients with high MMP9 expression, which provides potential therapeutic targets in further combination therapy of BLC.

There are still several limitations to this study. Firstly, the sample size of the IHC analyses was relatively small, which may limit the generalizability of the findings. Secondly, the reliance on publicly available datasets, such as TCGA, while providing a rich resource, also introduces potential biases inherent in retrospective data analysis. Additionally, due to the objective restriction, the functional validation of the identified biomarkers, MMP9, was

not performed in vitro or in vivo, which is essential for establishing causality. Lastly, the study primarily focuses on the correlation between MMP9 expression and immune cell infiltration, and further research is needed to elucidate the underlying mechanisms and potential therapeutic applications. Despite these limitations, the study provides valuable insights into the role of MMP9 in the tumor microenvironment of bladder cancer.

We found out the TME-related genes in BLC with ESTIMATE algorithm through the functional enrichment analysis of BLC samples from TCGA database, and considered MMP9 to be a potential prognostic factor for BLC patients. The GSEA was performed, and immunohistochemistry together with multiplex fluorescence immunohistochemistry further verified the association between TICs and MMP9, which may provide a novel direction for researches in the role of MMP9 in TME and targeted therapy for BLC.

#### Acknowledgements

The doctoral students in this project were under the support of Southeast University Innovation Capability Enhancement Plan for Doctoral Students. We are grateful to the staff in Biobank of Zhongda Hospital Affiliated to Southeast University for technical assistance.

#### Author contributions

HG and MC designed the study, conducted the study and maintained the data; FF, TG W and ZHY analyzed the data and made the figures and revised the manuscript; MX W and WC L drafted the manuscript; all authors viewed the paper and approved the version of the manuscript.

#### Funding

Southeast University Innovation Capability Enhancement Plan for Doctoral Students (CXJU\_SEU 24228).

#### Data availability

No datasets were generated or analysed during the current study.

#### Declarations

#### Ethics approval and consent to participate

The research procedure was in accordance with the ethical standards of the Declaration of Helsinki and Istanbul. The study protocol involving human bladder tissues was approved by the local ethics committee of Zhongda Hospital Affiliated to Southeast University. Written informed consent was obtained from all patients.

#### Consent for publication

Not applicable.

#### Competing interests

The authors declare no competing interests.

Received: 24 September 2024 / Accepted: 7 January 2025

Published online: 16 January 2025

#### References

1. Antoni S, Ferlay J, Soerjomataram I, Znaor A, Jemal A, Bray F. Bladder cancer incidence and mortality: a global overview and recent trends. *Eur Urol*. 2017;71:96–108.
2. American Cancer Society. Key Statistics for Bladder Cancer. <https://www.cancer.org/cancer/types/bladder-cancer/about/key-statistics.html>. Accessed Jan 2, 2025.

3. DeGeorge KC, Holt HR, Hodges SC. Bladder Cancer: diagnosis and Treatment[J]. *Am Family Phys*. 2017;96(8):507–14.
4. Witjes JA, Comperat E, Cowan NC, et al. European Association of Urology. EAU guidelines on muscle-invasive and metastatic bladder cancer: summary of the 2013 guidelines. *Eur Urol*. 2014;65(4):778–92.
5. Wu D. Innate and adaptive immune cell metabolism in tumor microenvironment. *Adv Exp Med Biol*. 2017;1011:211–23.
6. Holzel M, Bovier A, Tuting T. Plasticity of tumour and immune cells: a source of heterogeneity and a cause for therapy resistance? *Nat Rev Cancer*. 2013;13(5):365–76.
7. Wood SL, Pernemalm M, Crosbie PA, Whetton AD. The role of the tumor-microenvironment in lung cancer-metastasis and its relationship to potential therapeutic targets. *Cancer Treat Rev*. 2014;40:558–66. <https://doi.org/10.1016/j.ctrv.2013.10.001>.
8. Michael P, Maclean H, Autumn J, et al. Expansion of tumor infiltrating lymphocytes (TIL) from bladder cancer[J]. *Oncol Immunology*. 2017;7:1–7.
9. Gordon SR, Maute RL, Dulken BW, et al. PD-1 expression by tumour-associated macrophages inhibits phagocytosis and tumour immunity. *Nature*. 2017;545(7655):495–9.
10. Crispin PL, Kusmartsev S. Mechanisms of immune evasion in bladder cancer[J]. *Cancer Immunol Immunother*. 2019;69(4).
11. Ravi A, Garg P, Sitaraman SV. Matrix metalloproteinases in inflammatory bowel disease: boon or a bane? *Inflamm Bowel Dis*. 2007;13:97–107.
12. Deryugina EI, Zajac E, Juncker-Jensen A, Neoplasia et al. (New York, N.Y.), 2014, 16(10):771–88.
13. Rao Q, Chen Y, Yeh CR et al. Recruited mast cells in the tumor microenvironment enhance bladder cancer metastasis via modulation of ERβ/CCL2/CCR2 EMT/MMP9 signals[J]. *Oncotarget*. 2016;7(7).
14. Cancer Genome Atlas Research Network. Comprehensive molecular characterization of urothelial bladder carcinoma. *Nature*. 2014;507(7492):315–22.
15. Yoshihara K, Shahmoradgoli M, Martinez E, et al. Inferring tumour purity and stromal and immune cell admixture from expression data[J]. *Nat Commun*. 2013;4:2612.
16. Ashburner M, Ball CA, Blake JA, et al. Gene ontology: tool for the unification of biology. The Gene Ontology Consortium. *Nat Genet*. 2000;25(1):25–9.
17. Kanehisa M, Goto S. KEGG: kyoto encyclopedia of genes and genomes. *Nucleic Acids Res*. 2000;28(1):27–30.
18. Szklarczyk D, Gable AL, Lyon D, et al. STRING v11: protein-protein association networks with increased coverage, supporting functional discovery in genome-wide experimental datasets. *Nucleic Acids Res*. 2019;47(D1):D607–13.
19. Shannon P, Markiel A, Ozier O, et al. Cytoscape: a software environment for integrated models of biomolecular interaction networks. *Genome Res*. 2003;13(11):2498–504.
20. Newman AM, Liu CL, Green MR, et al. Robust enumeration of cell subsets from tissue expression profiles. *Nat Methods*. 2015;12(5):453–7.
21. Bergers G, Benjamin LE. Tumorigenesis and the angiogenic switch[J]. *Nat Rev Cancer*. 2003;3:401–10.
22. Deryugina EI, Quigley JP. Pleiotropic roles of matrix metalloproteinases in tumor angiogenesis: contrasting, overlapping and compensatory functions[J]. *Biochim Biophys Acta*. 2010;1803(1):103–20.
23. Quail DF, Joyce JA. Microenvironmental regulation of tumor progression and metastasis[J]. *Nat Med*. 2013;19(11):1423–37.
24. Mariathasan S, Turley SJ, Nickles D et al. TGF-β signalling attenuates tumour response to PD-L1 checkpoint blockade by contributing to retention of T cells in the peritumoural stroma[J]. *Ann Oncol*. 2017;28(suppl\_11).
25. Cumberbatch MGK, Jubber I, Black PC et al. Epidemiology of bladder Cancer: a systematic review and contemporary update of risk factors in 2018[J]. *Eur Urol*. 2018;74.
26. McConkey DJ, Choi W, Ochoa A, Dinney CPN. Intrinsic subtypes and bladder cancer metastasis. *Asian J Urol*. 2016;3:260–7.
27. Scannevin RH, Alexander R, Haarlander TM, et al. Discovery of a highly selective chemical inhibitor of matrix metalloproteinase-9 (MMP-9) that allosterically inhibits zymogen activation. *J Biol Chem*. 2017;292(43):17963–74.
28. Reggiani F, Labanca V, Mancuso P, et al. Adipose progenitor cell secretion of GM-CSF and MMP9 promotes a stromal and immunological microenvironment that supports breast Cancer Progression. *Cancer Res*. 2017;77(18):5169–82.
29. Mehner C, Hockla A, Miller E, Ran S, Radisky DC, Radisky ES. Tumor cell-produced matrix metalloproteinase 9 (MMP-9) drives malignant progression and metastasis of basal-like triple negative breast cancer. *Oncotarget*. 2014;5:2736–49.
30. Lyu X, Wang P, Qiao Q, Jiang Y. Genomic stratification based on microenvironment immune types and PD-L1 for tailoring therapeutic strategies in bladder cancer. *BMC Cancer*. 2021;21(1):646. <https://doi.org/10.1186/s12885-021-08350-1>. PMID: 34059019; PMCID: PMC8166145.
31. Subramanian A, Tamayo P, Mootha VK, et al. Gene set enrichment analysis: a knowledge-based approach for interpreting genome-wide expression profiles. *Proc Natl Acad Sci U S A*. 2005;102(43):15545–50.

## Publisher's note

Springer Nature remains neutral with regard to jurisdictional claims in published maps and institutional affiliations.